

## ORIGINAL ARTICLE

Relaxor-like behaviors in  $\text{Na}_{1/2}\text{Bi}_{1/2}\text{Cu}_3\text{Ti}_4\text{O}_{12}$  ceramicsChunchang Wang<sup>1</sup> | Wei Ni<sup>1</sup> | Xiaohong Sun<sup>1</sup> | Le Wang<sup>2</sup> | Can Wang<sup>2</sup> | Kuijuan Jin<sup>2</sup><sup>1</sup>Laboratory of Dielectric Functional Materials, School of Physics & Material Science, Anhui University, Hefei, China<sup>2</sup>Beijing National Laboratory for Condensed Matter Physics, Institute of Physics, Chinese Academy of Sciences, Beijing, China

## Correspondence

Chunchang Wang, Laboratory of Dielectric Functional Materials, School of Physics & Material Science, Anhui University, Hefei, China.  
Email: ccwang@ahu.edu.cn

## Funding information

National Natural Science Foundation of China, Grant/Award Number: 51572001 and 11174355; Weak Signal-Detecting Materials and Devices Integration of Anhui University, Grant/Award Number: Y01008411.

## Abstract

Dielectric properties of  $\text{Na}_{1/2}\text{Bi}_{1/2}\text{Cu}_3\text{Ti}_4\text{O}_{12}$  ceramics were evaluated over the temperature range 300–720 K. Two relaxor-like dielectric anomalies were found. The low-temperature anomaly was confirmed to be an oxygen-vacancy-related relaxation process. It is a pseudo-relaxor behavior caused by a bulk relaxation and a Maxwell-Wagner relaxation. The high-temperature one was evidenced to be an electric ferroelectric phase-transition process resulting from the oxygen-vacancy ordering.

## KEYWORDS

dielectric relaxation, electronic ferroelectricity,  $\text{Na}_{1/2}\text{Bi}_{1/2}\text{Cu}_3\text{Ti}_4\text{O}_{12}$  ceramics, relaxor

## 1 | INTRODUCTION

Relaxor ferroelectrics (RFs) are of significant technological and scientific interest, because they show striking phenomena such as piezoelectric, dielectric, ferroelectric, and electric-mechanical properties.<sup>1,2</sup> The well-known RF family is the lead-based B-site complex perovskites, such as  $\text{Pb}(\text{Mg}_{1/3}\text{Nb}_{2/3})\text{O}_3$ ,  $\text{Pb}(\text{Zr}_x\text{Ti}_{1-x})\text{O}_3$ , and so on. The toxic nature of PbO strongly limits their wide applications, which triggers a keen interest in developing new lead-free RF materials in recent years.<sup>3</sup> A number of Pb-free RFs, such as  $(\text{Bi}_{1/2}\text{Na}_{1/2})\text{TiO}_3$ ,<sup>4</sup>  $(\text{Na}_{1/2}\text{K}_{1/2})\text{NbO}_3$ ,<sup>5</sup> etc., were achieved in A-site complex perovskites leading to the empirical rule that the A-site complex perovskites might be candidates for the environmental friendly RFs.

Recently, the A-site complex perovskite  $\text{CaCu}_3\text{Ti}_4\text{O}_{12}$ , that is,  $(\text{Ca}_{1/4}\text{Cu}_{3/4})\text{TiO}_3$  (CCTO), has attracted extensive studies because of its weak temperature-dependent colossal dielectric constant (CDC,  $\epsilon' \sim 10^5$ ).<sup>6</sup> Although ferroelectric transition is physically prohibited in CCTO as it exhibits a centrosymmetric structure in a wide temperature range from 35 to 1273 K,<sup>7</sup> relaxor behavior was widely reported in

CCTO at high temperatures (350–600 K).<sup>8–14</sup> This behavior was ascribed to be caused by charge ordering<sup>11,15</sup> known as electronic ferroelectricity.<sup>16</sup> Our recent work revealed that this relaxor behavior is an extrinsic phenomenon related to oxygen vacancies.<sup>7</sup> This behavior is now called pseudo-relaxor behavior,<sup>17</sup> which is composed of two close relaxations with the low-temperature one being a dipolar relaxation and the high-temperature one being a Maxwell-Wagner relaxation.<sup>7</sup>

$\text{Na}_{1/2}\text{Bi}_{1/2}\text{Cu}_3\text{Ti}_4\text{O}_{12}$  (NBCTO) is isostructural with CCTO showing similar CDC behavior to that of CCTO in the temperature range below room temperature.<sup>18–21</sup> And, similar to Mn-doped CCTO,<sup>22</sup> both pure and Mn-doped NBCTO also shows incipient ferroelectricity.<sup>23,24</sup> The closely resembling low-temperature dielectric properties strongly suggest that both materials should possess similar high-temperature dielectric properties. Truly, a high-temperature relaxor-like behavior was recently reported in NBCTO. This behavior was ascribed to be a pseudo-relaxor behavior.<sup>25</sup> This prompts us to perform detailed studies on this question.

In this work, we reported the results of our studies on the high-temperature dielectric properties of NBCTO. Our

results show that, apart from the pseudo-relaxor behavior, an electric ferroelectric phase-transition process was also observed.

## 2 | EXPERIMENTAL PROCEDURE

NBCTO pellets used for dielectric measurements, were prepared by solid-state reaction using high-purity (99.99%) starting powders of  $\text{Na}_2\text{CO}_3$ ,  $\text{Bi}_2\text{O}_3$ ,  $\text{CuO}$ , and  $\text{TiO}_2$ . Stoichiometric amount of the powders were thoroughly mixed using a mortar and calcined at  $950^\circ\text{C}$  for 6 hours and  $1000^\circ\text{C}$  for 7.5 hours with intermediate grinding. Then, the mixture was reground and pressed into pellets with the size of 12 mm diameter and about 1-2 mm thickness under a pressure of 20 MPa and finally sintered at  $1050^\circ\text{C}$  for 6 hours at a heating rate of  $3^\circ\text{C}/\text{min}$  followed by furnace cooling. Phase purity of the sintered pellets was characterized by X-ray powder diffraction (XRD) on a Rigaku SmartLab diffractometer (Rigaku Beijing Co., Beijing, China) with  $\text{CuK}\alpha$  radiation. Microstructure and grain size of the sintered pellets were studied by a field-emission scanning electron microscope (SEM) (Model S-4 800, Hitachi Co. Ltd, Tokyo, Japan). Dielectric properties were obtained using a Wayne Kerr 6500B precise impedance analyzer (Wayne Kerr Electronic Instrument Co., Shenzhen, China) with the sample mounted in a holder placed inside a [PST-2000HL dielectric measuring system \(Partulab Co., Wuhan, China\)](#). The electrodes were made by printing silver paste on both sides of the disk-type samples and then fired at  $800^\circ\text{C}$  for 2 hours to remove the polymeric component before measuring. The ferroelectric properties were investigated using an RT6000 ferroelectric tester (Radiant Technologies Inc., Albuquerque, NM, USA) at room temperature. Annealing treatments were performed in flowing (200 mL/min)  $\text{O}_2$  and  $\text{N}_2$  (both with purity  $>99.999\%$ ) at  $800^\circ\text{C}$  for 2 hours.

## 3 | RESULTS AND DISCUSSION

Figure 1 shows the XRD pattern of a sintered sample. The pattern can be completely indexed based on the body centered cubic with the space group  $\text{Im}3$  according to JCPDS #75-2 188. Inset of Figure 1 displays the SEM surface morphology image of the sample, which reveals a condensed sintering nature. Relative density is 93.7% of the theoretical density, as determined by Archimedes method.

The temperature dependence ( $T$ ) of the dielectric constant,  $\varepsilon'(T)$ , and loss tangent,  $\tan\delta(T)$ , recorded under different frequencies for NBCTO sample were given in Figure 2A,B, respectively. It is clearly seen that there are two dielectric anomalies within the measuring temperature

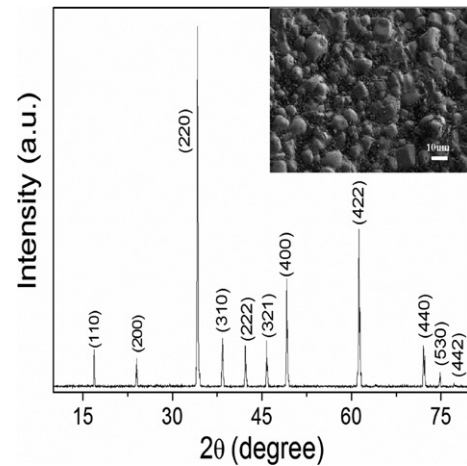


**FIGURE 1** XRD pattern of NBCTO pellet recorded at room temperature. The inset shows the SEM image for the pellet

range. For brevity, these anomalies were named as A1 and A2 in the order of ascending temperature. The position of each anomaly moves to higher temperature while its peak intensity decreases as the measuring frequency increases. This is the typical feature for a relaxor behavior. However, similar to the behavior reported by Liang et al.,<sup>25</sup> the  $\tan\delta$ - $T$  curves reveal a set of thermally activated relaxation peaks corresponding to A1. This fact indicates that the first anomaly is associated with a relaxation process rather than a ferroelectric phase transition. The relaxation parameters can be obtained in terms of the Arrhenius law:

$$f = f_0 \exp(-E_{\text{relax}}/k_B T_p) \quad (1)$$

where  $f_0$  is the pre-exponential factor,  $E_{\text{relax}}$  is the activation energy for relaxation,  $k_B$  is the Boltzmann constant, and  $T_p$  is the temperature where the maximum  $\tan\delta(T)$  occurs. The Arrhenius plot was shown in the inset of Figure 2B. The activation energy and pre-exponential factor were deduced to be 0.42 eV and  $2.75 \times 10^9$  Hz, respectively. The activation energy value agrees well with that caused by singly ionized oxygen vacancies, which was reported in the range of 0.3-0.5 eV.<sup>26-29</sup> It indicates that A1 might be associated with oxygen vacancies, which will be discussed in more detail later.

On the contrary, A2 was found to be accompanied by a set of humps in the curves of  $\tan\delta(T)$ . The humps are actually another set of peaks, which are almost merged by the rapidly increasing background in the temperature of  $T > 550$  K. The peak position hardly changes with frequency. To accurately clarify the peak position, one Debye peak superimposed on an exponentially increasing background with the form of  $a + b \exp(T/c)$  (with  $a$ ,  $b$ , and  $c$  being the adjustable parameters) were adopted to fit the experimental data of the loss tangent. As a representative

example, the resulting Debye peak and background for the experimental data measured at 500 Hz were shown in Figure 2C. Perfect agreement between the experimental data and the fitting result was achieved. The inset of Figure 2C displays the resulting peaks at different frequencies, which truly reveals that the peak position is independent of the measuring frequency. This finding indicates that the anomaly A2 is associated with a relaxor phase-transition process. The transition temperature,  $T_t$ , is identified to be 525 K. This behavior is quite different from the one reported by Liang et al.,<sup>25</sup> indicating that the present one is a new anomaly.

To decipher the nature of these anomalies, we will discuss them separately in the following. We first focus on A1. Since the change in Cu valence plays an important role in determining the CDC behavior in CCTO,<sup>30</sup> one may anticipate that A1 might be associated with the change in Cu valence. This possibility can be ruled out because A1 was also found in NBCTO samples with either 10 mol% Bi or Na-overdosed (results not shown). The change in Cu valence in the overdosed samples was not observed.<sup>21</sup> As already confirmed that A1 is a relaxation process, it might be a pseudo-relaxor behavior which can be induced by either the negative capacitance effect<sup>31,32</sup> or the aforementioned two-relaxation model.<sup>7</sup> The absence of the negative capacitance effect indicates that the two-relaxation model might account for A1. If so, the anomaly should be composed of two oxygen-vacancy related relaxations. To confirm this reference, we measured the dielectric properties on the NBCTO pellet after being annealed first in O<sub>2</sub> and then in N<sub>2</sub>. The dielectric parameters recorded at 300 Hz in the as-prepared, O<sub>2</sub>- and N<sub>2</sub>-annealed cases were summarized in Figure 2D. From which we can see that A1 can be greatly depressed by the O<sub>2</sub>-annealing treatment and then enhanced by the N<sub>2</sub>-annealing treatment. This finding substantially confirms that A1 is related to oxygen vacancies.

Figure 3 compares the enlarged view of the  $\tan\delta(T)$  peak recorded at 300 Hz in the as-prepared, O<sub>2</sub>- and N<sub>2</sub>-annealed cases. Likewise, the  $\tan\delta(T)$  curve is notably depressed by the O<sub>2</sub>-annealing treatment and then enhanced by the N<sub>2</sub>-annealing treatment. In the O<sub>2</sub>-annealed case, apart from a small peak around 340 K, a weak hump at about 430 K can be well identified. This finding implies that the broad peak in the as-prepared and N<sub>2</sub>-annealed cases is composed of two close relaxation peaks. Thus, two relaxation peaks superimposed on an exponentially increasing background were used to fit the  $\tan\delta(T)$  peak. The fitting curves (solid lines) and the resulting peaks (dashed curves) for all cases were present in the figure. Perfect fitting results were obtained confirming that the  $\tan\delta(T)$  peak contains two relaxation processes. These results convince that the low-temperature dielectric anomaly A1 is a pseudo-relaxor behavior. Pseudo-relaxor behavior caused

by two oxygen-vacancy-relaxation relaxations is a rather ubiquitous effect in oxides, being often observed at high enough temperature.<sup>7</sup> The low- and high-temperature relaxations were identified to be bulk and Maxwell-Wagner relaxations, respectively.<sup>7</sup> The bulk relaxation is induced by the hopping motions of singly ionized oxygen vacancies. When the vacancies are blocked by grain boundaries, the Maxwell-Wagner relaxation ensues.

We now turn our attention to the nature of the high-temperature dielectric anomaly A2. It was suggested to be a relaxor phase-transition process. A characteristic feature for a relaxor is that the dielectric behavior in the temperature range of  $T > T_m$  (where  $T_m$  is the peak temperature) can be described by the modified Curie-Weiss law,<sup>33</sup> which is expressed as:

$$\frac{1}{\epsilon'} - \frac{1}{\epsilon'_{\max}} = C(T - T_m)^\alpha \quad (2)$$

where  $\epsilon'_{\max}$  is the dielectric constant at the peak temperature,  $C$  and  $\alpha$  are modified constants. The power factor  $\alpha$  with the value between 1 and 2 gives the character of the ferroelectric phase transition. The limiting values 1 and 2 correspond to a normal ferroelectric and an ideal ferroelectric relaxor, respectively.<sup>34</sup> According to Equation (2) there is a linear relationship between  $\ln(1/\epsilon' - 1/\epsilon'_{\max})$  and  $\ln(T - T_m)$ . Figure 4A presents such plot for the curve recorded under 500 Hz. As expected, a good linear relationship was obtained. Linear fittings yield the values of the power factor under different frequencies, which were shown in Table 1. The  $\alpha$  values are close to 2 indicating that NBCTO is close to a relaxor ferroelectric.

Another characteristic feature for a relaxor is that the  $T_m$  obeys the Vogel-Fulcher (VF) law<sup>35</sup>

$$f = f_0 \exp\{-E/[k_B(T_m - T_{VF})]\} \quad (3)$$

where  $E$  is the barrier energy,  $T_{VF}$  is the Vogel-Fulcher temperature. Figure 4B displays the plot of  $f$  as a function of  $T_m$ . The data can be well fitted by the VF law. The fitting yields  $f_0 = 9.9327 \times 10^5$  Hz,  $E = 0.0204$  eV and  $T_{VF} = 519.4774$  K. These values are comparable with those found in TiO<sub>2</sub> polymorphs.<sup>36</sup> This fact further indicates the relaxor nature of the high-temperature anomaly.

An indispensable feature for relaxor ferroelectrics is the polarization-electric field loop. Figure 4D shows the room-temperature polarization loop recorded under 1 kHz. A clear hysteresis loop was observed. The loop is not saturated indicative of a lossy loop or banana loop as coined by Scott.<sup>37</sup> Although, the loop is not always a reliable evidence to identify a ferroelectric or relaxor behavior, it reveals the lossy natured behavior for NBCTO. The loss can be reasonably ascribed to the conductivity contribution

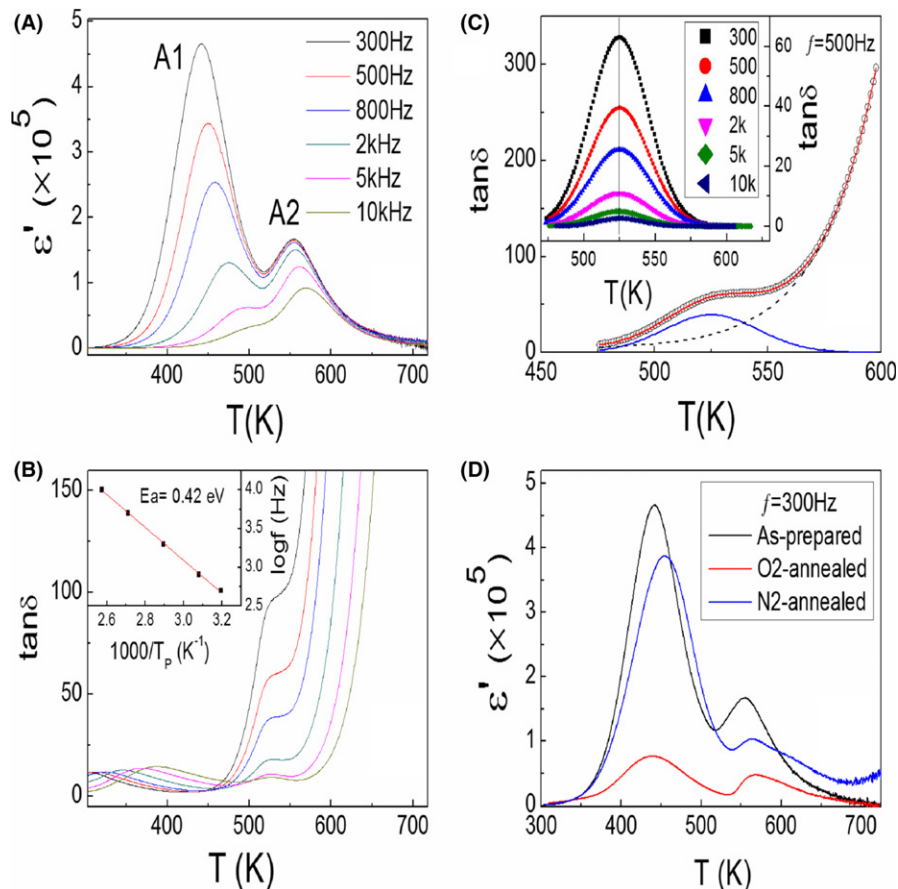


**FIGURE 2** (A) and (B) Temperature dependence of dielectric constant and loss tangent, respectively. The inset in (B) shows the Arrhenius plot of the relaxation peak. (C) A representative result of the least-square fit to the experimental data obtained at 500 Hz. The inset in (C) shows the resulting peaks at different frequencies. The vertical line indicates the phase-transition temperature. (D) Comparison of the temperature dependence of  $\tan\delta(T)$  obtained at 300 Hz for a NBCTO sample in the as-prepared,  $O_2$ - and  $N_2$ -annealed cases [Color figure can be viewed at [wileyonlinelibrary.com](http://wileyonlinelibrary.com)]

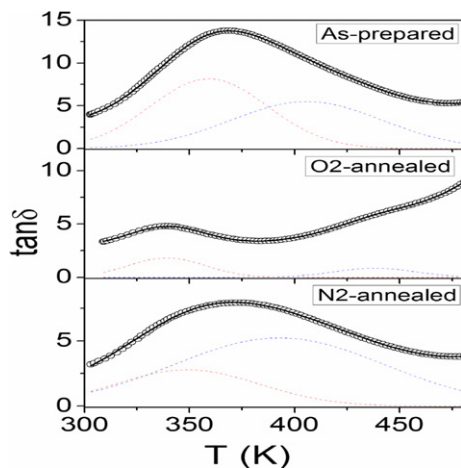


**FIGURE 3** The two-relaxation process fitting results for the  $\tan\delta(T)$  peak at 300 Hz in the as-prepared,  $O_2$ - and  $N_2$ -annealed cases [Color figure can be viewed at [wileyonlinelibrary.com](http://wileyonlinelibrary.com)]

due to oxygen vacancies as already confirmed that oxygen vacancies dominate the high-temperature dielectric properties of NBCTO. This raises the fundamental question of the origin of the ferroelectric behavior in NBCTO, because the centrosymmetric structure prohibits the conventional ferroelectric behavior, which involves a *change in crystal structure*.<sup>38</sup> Thanks to the revival of interest in multiferroic materials, breakthrough in ferroelectric theory came in the

**TABLE 1** VF fitting results for A2

Frequency (Hz)	$T_m$ (K)	$\frac{1}{\epsilon'_{max}} (10^{-6})$	$\alpha$
500	555	6.06	1.948
2000	557	6.64	1.961
5000	561	8.01	1.954

early 1990s, and a number of alternative mechanisms for ferroelectricity had been revealed. Mechanisms found to date include the incorporation of stereochemically active lone pair cations, for example, in  $BiMnO_3$  and  $BiFeO_3$ <sup>39,40</sup>; geometric ferroelectricity in  $YMnO_3$ ,  $BaNbF_4$ , and related compounds<sup>41,42</sup>; charge ordering, as in  $LuFeO_3$ <sup>43,44</sup>; and polar magnetic spin-spiral states in  $RMnO_3$  ( $R=Gd, Tb, Dy, Ho$ ).<sup>45-47</sup> Among them, the charge-ordering-induced ferroelectricity, also named as electric ferroelectricity, is almost a common dielectric phenomenon in transition-metal oxides. This mechanism involves a *change in electronic structure* which breaks the space-inversion symmetry giving rise to a macroscopic polarization.<sup>48,49</sup> Since oxygen vacancies are the predominant charge carriers in the high-temperature range, it is natural to anticipate that the observed relaxor behavior might be related to the oxygen-vacancy-ordering. Evidence supporting this inference comes from the thermal analysis. Since the process of

oxygen vacancies change from disordered to ordered states belongs to a weak first-order phase transition. This process should be accompanied by an exothermic peak in the differential scanning calorimetry (DSC) curve. Figure 3D displays the DSC result for NBCTO. We truly found a broad exothermic peak locating around 466 K. The peak temperature is lower than the phase-transition temperature  $T_i$  (525 K). This is because that  $T_i$  is size-dependent.<sup>50</sup> The DSC measurement requires the bulk ceramic sample to be ground into powders. The reduced grain size leads to the decrease of  $T_c$ .

Thus, it follows that the second dielectric anomaly (A2) is associated with a relaxor phase transition caused by oxygen-vacancy ordering. A pertinent question is that why only the pseudo-relaxor behavior was observed by Liang and coauthors? The size-dependent feature of true relaxor behavior provides a heuristic hint to the question. To clarify this point, a new NBCTO pellet with the original thickness of  $t=1.46$  mm was used. Dielectric measurements were performed after reducing the thickness by evenly polishing the pellet from both sides down to  $t=1.14$  and 0.8 mm. Figure 5 compares the dielectric constant (left panels) and corresponding loss tangent (right panels) for the pellet by reducing its thicknesses down to different values. It is clearly seen that, when  $t=1.46$  mm

(Figure 4A,B), the pellet shows only one dielectric anomaly accompanied by a set of relaxation peaks in the curves of  $\tan\delta(T)$ . Compared with the results presented in Figure 1, this anomaly can be identified to be A1. When the thickness was reduced to 1.14 mm (Figure 5C,D), apart from A1, which becomes much smaller than that of the original state, another weak anomaly appears in the temperature around 600 K. Correspondingly, a set of notable phase-transition-like peaks occur in  $\tan\delta(T)$ . Obviously, this anomaly is A2. The phase-transition temperature is found to be 555 K. The inset of Figure 5D is the enlarged view of the rectangle area, which clearly shows a set of relaxation peaks. When  $t$  is reduced to 0.8 mm (Figure 5E,F), A1 further decreases in intensity, A2 almost behaves as a step-like increase due to the remarkable background in the temperature above 600 K. But the phase-transition-like peaks in  $\tan\delta(T)$  are still notable. The phase-transition temperature reduces to 516 K. This finding confirms that the relaxor phase-transition is size-dependent. That is to say, the thicker of the sample, the higher temperature of the phase-transition. Since the high-temperature dielectric properties are dominated by the conductivity, which induces strongly increasing background as revealed in Figure 5B, the signal of the phase-transition would be completely shadowed. This might be the reason

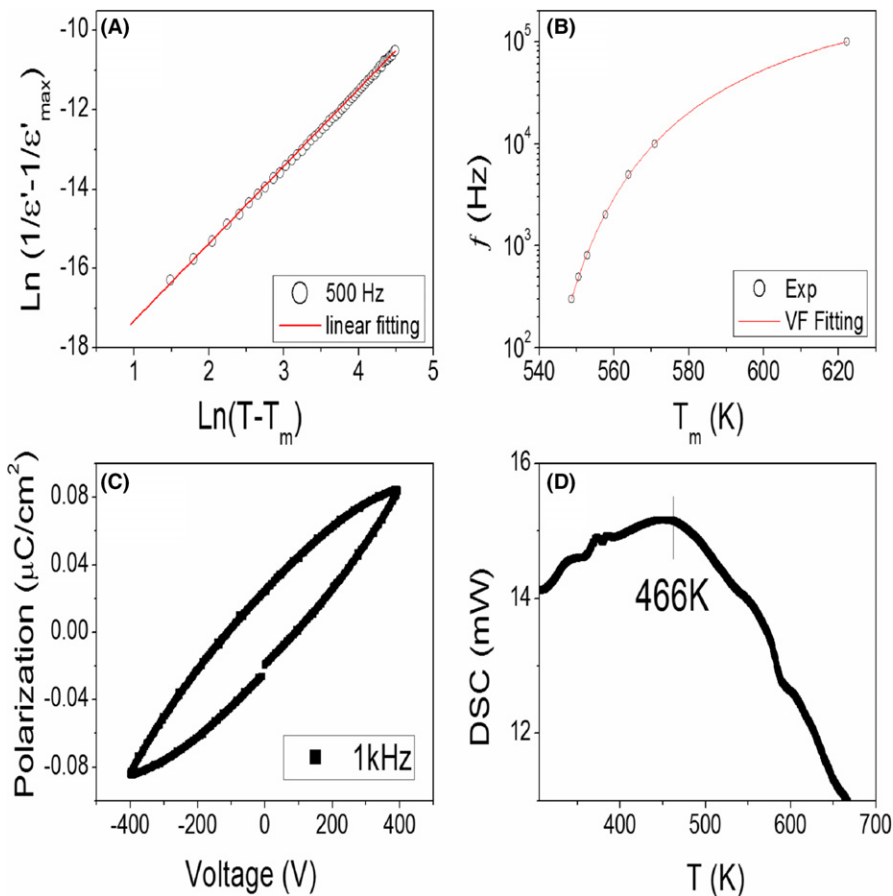


**FIGURE 4** A, The plot of  $\ln(1/\epsilon' - 1/\epsilon'_{\max})$  as a function of  $\ln(T - T_m)$  for the data obtained at 500 Hz. B, The VF fitting to the anomaly position of A2. C, The polarization hysteresis loop of NBCTO. D, The DSC curve of NBCTO [Color figure can be viewed at [wileyonlinelibrary.com](http://wileyonlinelibrary.com)]

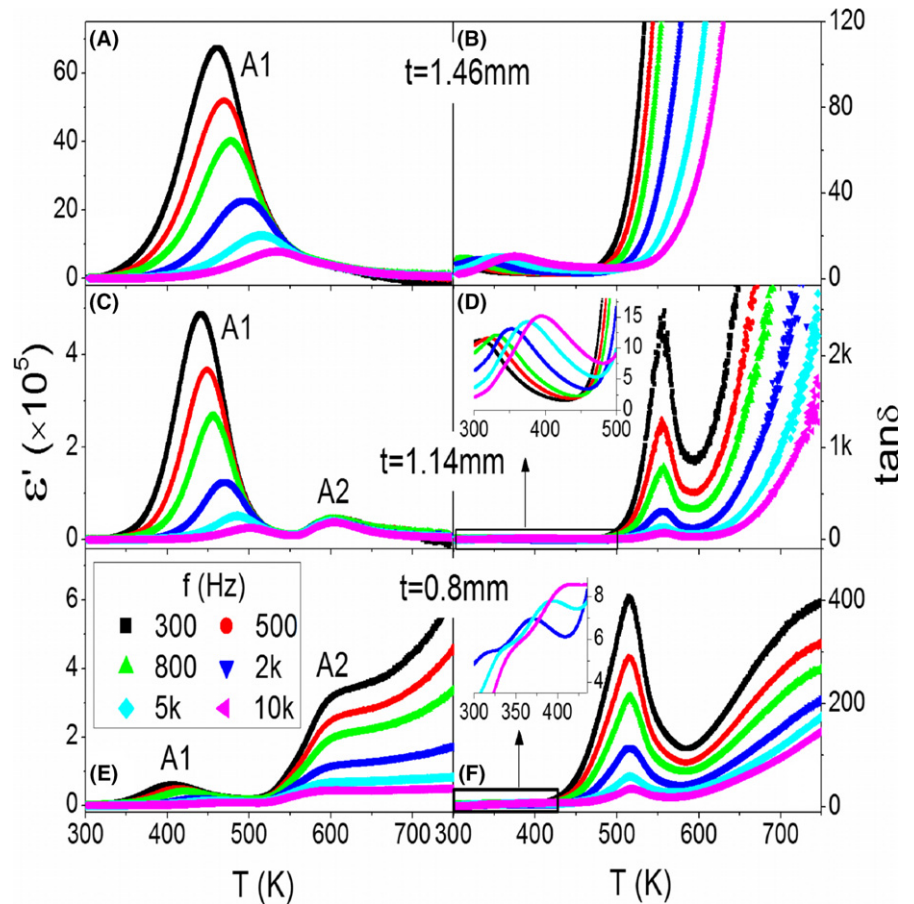


**FIGURE 5** Temperature dependence of dielectric constant (left panels) and loss tangent (right panels) for a new NBCTO sample after being polished to various thicknesses [Color figure can be viewed at [wileyonlinelibrary.com](http://wileyonlinelibrary.com)]

why Liang et al. only found the pseudo-relaxor behavior. More interestingly, an enlarged view of the low-temperature  $\tan\delta(T)$  (Inset of Figure 5F. For clarity, only the curves recorded 2, 5, and 10 kHz were displayed) clearly reveals two sets of relaxation peaks. This finding substantially demonstrates that A1 truly contains two relaxation processes and confirms the two-relaxation mechanism for A1.

Finally, it is worth emphasizing that the size effect is a typical feature for conventional ferroelectricity when the grain size (for bulk) or sample thickness (for film) is reduced down to nanoscaled region.<sup>50</sup> In the present case, either the grain size or sample thickness is much larger than the region. The strong size effect of the electric ferroelectricity in NBCTO can be reasonably explained by considering the fact that the reduction in sample thickness is actually the enhancement of the applied electric field. It was reported that a small electric field could effectively affect the charge ordering leading to a larger dielectric tunability.<sup>51</sup> A dielectric tunability of 71.43% achieved at 800 Hz and 303 K under an electric field of 200 V/cm was found the NBCTO. Details about the dielectric tunability will be present in an ensuing paper.<sup>52</sup> This result also suggests a facile way to tune the charge ordering via electric field.

## 4 | CONCLUSIONS

In conclusion, we have investigated the high-temperature (300–720 K) dielectric properties of  $\text{Na}_{1/2}\text{Bi}_{1/2}\text{Cu}_3\text{Ti}_4\text{O}_{12}$  ceramic samples. Two relaxor-like anomalies were observed. The low-temperature anomaly was ascribed to be a pseudo-relaxor behavior resulting from the combination of a bulk relaxation and a Maxwell-Wagner relaxation. The high-temperature one was confirmed to be associated with a relaxor phase transition caused by oxygen-vacancy ordering.

## ACKNOWLEDGMENTS

The authors thank financial support from National Natural Science Foundation of China (Grant Nos. 51572001 and 11174355). This work was supported in part by the Weak Signal-Detecting Materials and Devices Integration of Anhui University (Grant No. Y01008411).

## REFERENCES

- Smolensky GA, Agranovskaya AI. Dielectric polarization and losses of some complex compounds. *Sov Phys Solid State*. 1959;10:1429–1437.

2. Chaisan W, Yimnirun R, Ananta S, Cann DP. Dielectric properties of solid solutions in the lead zirconate titanate-barium titanate system prepared by a modified mixed-oxide method. *Mater Lett.* 2005;59:3732–3737.
3. Cross LE. Materials science: lead-free at last. *Nature.* 2004;432:24–25.
4. Sun H, Peng D, Wang X, Tang M, Zhang Q, Yao X. Strong red emission in Pr doped  $(\text{Bi}_{0.5}\text{Na}_{0.5})\text{TiO}_3$  ferroelectric ceramics. *J Appl Phys.* 2011;110:016102. 3pp.
5. Ahn ZS, Schulze WA. Conventionally sintered  $(\text{Na}_{0.5}, \text{K}_{0.5})\text{NbO}_3$  with barium additions. *J Am Ceram Soc.* 1987;70:C18–C21.
6. Homes CC, Vogt T, Shapiro SM, Wakimoto S, Ramirez AP. Optical response of high-dielectric-constant perovskite-related oxide. *Science.* 2001;293:673–676.
7. Wang CC, Zhang MN, Xu KB, Wang GJ. Origin of high-temperature relaxor-like behavior in  $\text{CaCu}_3\text{Ti}_4\text{O}_{12}$ . *J Appl Phys.* 2012;112:034109. 7pp.
8. Wang CC, Zhang LW. Oxygen-vacancy-related dielectric anomaly in  $\text{CaCu}_3\text{Ti}_4\text{O}_{12}$ : post-sintering annealing studies. *Phys Rev B.* 2006;74:024106. 4pp.
9. Ke SM, Huang HT, Fan HQ. Relaxor behavior in  $\text{CaCu}_3\text{Ti}_4\text{O}_{12}$  ceramics. *Appl Phys Lett.* 2006;89:182904. 3pp.
10. Yu HT, Liu HX, Hao H, et al. Grain size dependence of relaxor behavior in  $\text{CaCu}_3\text{Ti}_4\text{O}_{12}$  ceramics. *Appl Phys Lett.* 2007;91:222911. 3pp.
11. Prakash BS, Varma KBR. Ferroelectriclike and pyroelectric behavior of  $\text{CaCu}_3\text{Ti}_4\text{O}_{12}$  ceramics. *Appl Phys Lett.* 2007;90:082903. 3pp.
12. Onodera A, Kawatani K, Takesada M, Oda M, Ido M. Dielectric and thermal properties of single-crystalline  $\text{CaCu}_3\text{Ti}_4\text{O}_{12}$  at high temperatures. *Jpn J Appl Phys.* 2009;Part 1 48:09KF12.
13. Onodera A, Takesada M, Kawatani K, Hiramatsu S. Dielectric properties and phase transition in  $\text{CaCu}_3\text{Ti}_4\text{O}_{12}$  at high temperatures. *Jpn J Appl Phys.* 2008;Part 1 47:7753–7756.
14. Onodera A, Takesada M. Anomalous dielectric behavior in  $\text{CaCu}_3\text{Ti}_4\text{O}_{12}$  at high temperatures. *Ferroelectrics.* 2009;379:239–245.
15. Ni L, Chen XM. Dielectric relaxations and formation mechanism of giant dielectric constant step in  $\text{CaCu}_3\text{Ti}_4\text{O}_{12}$  ceramics. *Appl Phys Lett.* 2007;91:122905. 3pp.
16. Portengen T, Östreich T, Sham LJ. Theory of electronic ferroelectricity. *Phys Rev B.* 1996;54:17452–17463.
17. Wang CC, Dou SX. Pseudo-relaxor behaviour induced by Maxwell-Wagner relaxation. *Solid State Commun.* 2009;149:2017–2020.
18. Ferrarelli MC, Adams TB, Feteira A, Sinclair DC, West AR. High intrinsic permittivity in  $\text{Na}_{1/2}\text{Bi}_{1/2}\text{Cu}_3\text{Ti}_4\text{O}_{12}$ . *Appl Phys Lett.* 2006;89:212904. 3pp.
19. Ren HM, Liang PF, Yang ZP. Processing, dielectric properties and impedance characteristics of  $\text{Na}_{0.5}\text{Bi}_{0.5}\text{Cu}_3\text{Ti}_4\text{O}_{12}$  ceramics. *Mater Res Bull.* 2010;45:1608–1613.
20. Yang ZP, Ren HM, Chao XL, Liang PF. High permittivity and low dielectric loss of  $\text{Na}_{0.5}\text{Bi}_{0.5-x}\text{La}_x\text{Cu}_3\text{Ti}_4\text{O}_{12}$  ceramics. *Mater Res Bull.* 2012;47:1273–1277.
21. Sun XH, Wang CC, Wang GJ, Lei CM, Li T, Liu LN. Low-temperature dielectric relaxations associated with mixed-valent structure in  $\text{Na}_{0.5}\text{Bi}_{0.5}\text{Cu}_3\text{Ti}_4\text{O}_{12}$ . *J Am Ceram Soc.* 2013;96:1479–1503.
22. Li M, Feteira A, Sinclir DC, West AR. Incipient ferroelectricity and microwave dielectric resonance properties of  $\text{CaCu}_{2.85}\text{Mn}_{0.15}\text{Ti}_4\text{O}_{12}$  ceramics. *Appl Phys Lett.* 2007;91:132911. 3pp.
23. Ferrarelli MC, Sinclair DC, West AR. Possible incipient ferroelectricity in Mn-doped  $\text{Na}_{1/2}\text{Bi}_{1/2}\text{Cu}_3\text{Ti}_4\text{O}_{12}$ . *Appl Phys Lett.* 2009;94:212901. 3pp.
24. Ferrarelli MC, Nuzhnyy D, Sinclair DC, Kamba S. Soft-mode behavior and incipient ferroelectricity in  $\text{Na}_{1/2}\text{Bi}_{1/2}\text{Cu}_3\text{Ti}_4\text{O}_{12}$ . *Phys Rev B.* 2010;81:224112. 7pp.
25. Liang PF, Li YY, Chao XL, Yang ZP. Pseudo-relaxor behavior in  $\text{Na}_{1/2}\text{Bi}_{1/2}\text{Cu}_3\text{Ti}_4\text{O}_{12}$  ceramics. *Mater Res Bull.* 2014;60:212–216.
26. Peláiz-Barranco A, Guerra JDS. Dielectric relaxation related to single-ionized oxygen vacancies in  $(\text{Pb}_{1-x}\text{La}_x)(\text{Zr}_{0.90}\text{Ti}_{0.10})_{1-x/4}\text{O}_3$  ceramics. *Mater Res Bull.* 2010;45:1311–1313.
27. Bidault O, Goux P, Kchikech M, Belkaoui M, Maglione M. Space-charge relaxation in perovskites. *Phys Rev B.* 1994;49:7868–7873.
28. Ang C, Yu Z, Cross LE. Oxygen-vacancy-related low-frequency dielectric relaxation and electrical conduction in  $\text{Bi:SrTiO}_3$ . *Phys Rev B.* 2000;62:228–236.
29. Shulman HS, Damjanovic D, Setter N. Niobium doping and dielectric anomalies in bismuth titanate. *J Am Ceram Soc.* 2000;83:528–532.
30. Fang TT, Mei LT. Evidence of Cu deficiency: a key point for the understanding of the mystery of the giant dielectric constant in  $\text{CaCu}_3\text{Ti}_4\text{O}_{12}$ . *J Am Ceram Soc.* 2007;90:638–640.
31. Li M, Sinclair DC, West AR. Extrinsic origins of the apparent relaxor like behavior in  $\text{CaCu}_3\text{Ti}_4\text{O}_{12}$  ceramics at high temperatures: a cautionary tale. *J Appl Phys.* 2011;109:084106. 9pp.
32. Li M, Feteira A, Sinclair DC. Relaxor ferroelectric-like high effective permittivity in leaky dielectrics/oxide semiconductors induced by electrode effects: a case study of  $\text{CuO}$  ceramics. *J Appl Phys.* 2009;105:114109. 8pp.
33. Tian HY, Wang DY, Lin DM, Zeng JT, Kwok KW, Chan HLW. Diffusion phase transition and dielectric characteristics of  $\text{Bi}_{0.5}\text{Na}_{0.5}\text{TiO}_3\text{-Ba}(\text{Hf}, \text{Ti})\text{O}_3$  lead-free ceramics. *Solid State Commun.* 2007;142:10–14.
34. Victor P, Ranjith R, Krupanidhi SB. Normal ferroelectric to relaxor behavior in laser ablated Ca-doped barium titanate thin films. *J Appl Phys.* 2003;94:7702. 7pp.
35. Tagantsev AK. Stochastic process with ultraslow convergence to a Gaussian: the truncated Lévy flight. *Phys Rev Lett.* 1994;72:1100–1103.
36. Mani R, Achary SN, Chakraborty KR, et al.  $\text{FeTiTaO}_6$ : a lead-free relaxor ferroelectric based on the rutile structure. *Adv Mater.* 2008;20:1348–1352.
37. Scott JF. Ferroelectrics go bananas. *J Phys: Condens Matter.* 2008;20:021001. 2pp.
38. Lines M, Glass A. *Principles and Applications of Ferroelectrics and Related Materials.* Oxford: Clarendon; 1977.
39. Seshadri R, Hill NA. Visualizing the role of Bi 6s “Lone Pairs” in the off-center distortion in ferromagnetic  $\text{BiMnO}_3$ . *Chem Mater.* 2001;13:2892–2899.
40. Wang J, Neaton JB, Zheng H, et al. Epitaxial  $\text{BiFeO}_3$  multiferroic thin film heterostructures. *Science.* 2003;299:1719–1722.
41. van Aken BB, Pastra TTM, Filippetti A, Spaldin NA. The origin of ferroelectricity in magnetoelectric  $\text{YMnO}_3$ . *Nat Mater.* 2004;3:164–170.

42. Ederer C, Spaldin NA. Origin of ferroelectricity in the multiferroic barium fluorides BaMF<sub>4</sub>: a first principles study. *Phys Rev B*. 2006;74:024102. 8pp.
43. Ikeda N, Ohsumi H, Ohwada K, et al. Ferroelectricity from iron valence ordering in the charge-frustrated system LuFe<sub>2</sub>O<sub>4</sub>. *Nature*. 2005;436:1136–1138.
44. Subramanian MA, Tao H, Chen J, Ragado NS, Calverese TG, Sleight AW. Giant room-temperature magnetodielectric response in the electronic ferroelectric LuFe<sub>2</sub>O<sub>4</sub>. *Adv Mater*. 2006;18:1737–1739.
45. Kimura T, Goto T, Shintani H, Ishizaka K, Arima T, Tokura Y. Magnetic control of ferroelectric polarization. *Nature*. 2003;426:55–58.
46. Lottermoser Th, Lonkai T, Amann U, Hohlwein D, Ihringer J, Fiebig M. Magnetic phase control by an electric field. *Nature*. 2004;430:541–544.
47. Hemberger J, Lunkenheimer P, Fichtl R, Krug von Nidda HA, Tsurkan V, Loidl A. Relaxor ferroelectricity and colossal magnetocapacitive coupling in ferromagnetic CdCr<sub>2</sub>S<sub>4</sub>. *Nature*. 2005;434:364–367.
48. Sagayama H, Toyoda S, Sugimoto K, Maeda Y, Yamada S, Arima T. Ferroelectricity driven by charge ordering in the A-site ordered perovskite manganite SmBaMn<sub>2</sub>O<sub>6</sub>. *Phys Rev B*. 2014;90:241113(R). 4pp.
49. Yamauchi K, Barone P. Electronic ferroelectricity induced by charge and orbital orderings. *J Phys: Condens Matter*. 2014;26:103201.
50. Zhou Z, Buscaglia V, Viviani M, et al. Grain-size effects on the ferroelectric behavior of dense nanocrystalline BaTiO<sub>3</sub> ceramics. *Phys Rev B*. 2004;70:024107. 8pp.
51. Li CH, Zhang XQ, Cheng ZH, Suna Y. Room temperature giant dielectric tunability effect in bulk LuFe<sub>2</sub>O<sub>4</sub>. *Appl Phys Lett*. 2008;92:182903. 3pp.
52. Li QJ, Zhang ZP, Ni W, Sun XH, Wang CC. Large and switchable dielectric tunability in Na<sub>1/2</sub>Bi<sub>1/2</sub>Cu<sub>3</sub>Ti<sub>4</sub>O<sub>12</sub> ceramics. *J Alloy Compd*. 2017;695:1561–1565.

**How to cite this article:** Wang C, Ni W, Sun X, Wang L, Wang C, Jin K. Relaxor-like behaviors in Na<sub>1/2</sub>Bi<sub>1/2</sub>Cu<sub>3</sub>Ti<sub>4</sub>O<sub>12</sub> ceramics. *J Am Ceram Soc*. 2017;100:2016–2023.